AGU PUBLICATIONS

Geophysical Research Letters

RESEARCH LETTER

10.1002/2013GL058744

Key Point:
- Only few aftershocks inside stress shadows can be linked to secondary effects

Supporting Information:
- Readme
- Figure S1
- Figure S2
- Appendixes S1 and S2
- Table S1
- Table S2

Correspondence to:
M. Segou,
segou@geoazur.unice.fr

Citation:
Segou, M., and T. Parsons (2014), The stress shadow problem in physics-based aftershock forecasting: Does incorporation of secondary stress changes help?, *Geophys. Res. Lett.*, *41*, doi:10.1002/2013GL058744.

Received 2 APR 2014
Accepted 19 MAY 2014
Accepted article online 21 MAY 2014

The stress shadow problem in physics-based aftershock forecasting: Does incorporation of secondary stress changes help?

M. Segou[1,2] and T. Parsons[1]

[1]United States Geological Survey, Menlo Park, California, USA, [2]Now at GeoAzur/CNRS, Valbonne, France

Abstract Main shocks are calculated to cast stress shadows across broad areas where aftershocks occur. Thus, a key problem with stress-based operational forecasts is that they can badly underestimate aftershock occurrence in the shadows. We examine the performance of two physics-based earthquake forecast models (Coulomb rate/state (CRS)) based on Coulomb stress changes and a rate-and-state friction law for their predictive power on the 1989 $M_w = 6.9$ Loma Prieta aftershock sequence. The CRS-1 model considers the stress perturbations associated with the main shock rupture only, whereas CRS-2 uses an updated stress field with stresses imparted by $M \geq 3.5$ aftershocks. Including secondary triggering effects slightly improves predictability, but physics-based models still underestimate aftershock rates in locations of initial negative stress changes. Furthermore, CRS-2 does not explain aftershock occurrence where secondary stress changes enhance the initial stress shadow. Predicting earthquake occurrence in calculated stress shadow zones remains a challenge for stress-based forecasts, and additional triggering mechanisms must be invoked.

1. Introduction

Operational aftershock forecasting is usually based either on statistics derived from our empirical knowledge of the system [*Ogata*, 1998] or on physical models that anticipate seismicity by invoking rate-and-state friction laws combined with static stress change calculations [e.g., *Stein*, 1999; *Toda et al.*, 2005]. Researchers have not reached consensus on static stress change effects, suggesting, for example, that there is a strong spatial correlation between stress shadows and seismicity rate reduction [*Toda et al.*, 2012], a total absence of stress shadows [*Felzer and Brodsky*, 2005], or alteration of primary focal mechanisms [*Mallman and Parsons*, 2008]. Usually correlation between static stress increases and major historic earthquakes [*Stein*, 1999] and/or aftershocks considers just the main shock perturbation and long-term aftershock occurrence [e.g., *Toda and Stein*, 2003]. In the near-source region it is difficult to identify aftershocks triggered by static or dynamic stress changes because both are expected to increase seismicity rates [*Freed*, 2005; *Hill and Prejean*, 2007]. *Felzer and Brodsky* [2005] find distinct distance decay related to dynamically triggered aftershocks from earthquake sources with M2-6 [*Richards-Dinger et al.*, 2010]. More recently, *Parsons et al.* [2012] found that microseismicity patterns within aftershock sequences cannot be fully explained by main shock static stress changes, since they are partly caused from secondary triggering. *Marsan* [2005] suggested that, at large scale, an aftershock distribution is constrained by the early stress release and clustering inside stress increased regions, which does not evolve much through the sequence.

In this study we investigate whether continuous updating of the stress field by perturbations caused from smaller magnitude aftershocks ($M \geq 3.5$) improves the predictive power of forecast models based on a rate/state friction law and static stress changes. We compare the predictive power of two Coulomb rate/state (CRS) forecast models, the CRS-1 model, which considers the stress perturbations associated with the main shock rupture only, and the CRS-2 model, which corresponds to a time evolving stress field incorporating stresses imparted by aftershocks within three clusters near the epicentral region of 1989 Loma Prieta M_w 6.9 in Northern California. We then compare the number of forecasted events with $M \geq 1.6$ from both implementations with observations. Finally, we discuss how our results contribute in the development of future operational forecasting efforts and understanding earthquake triggering processes.

2. Data and Methods

There are two main characteristics that make the Loma Prieta aftershock sequence a compelling case study for secondary triggering studies: (1) aftershock clusters that initiated within the first 24–30 h after the main

©2014. American Geophysical Union. All Rights Reserved.

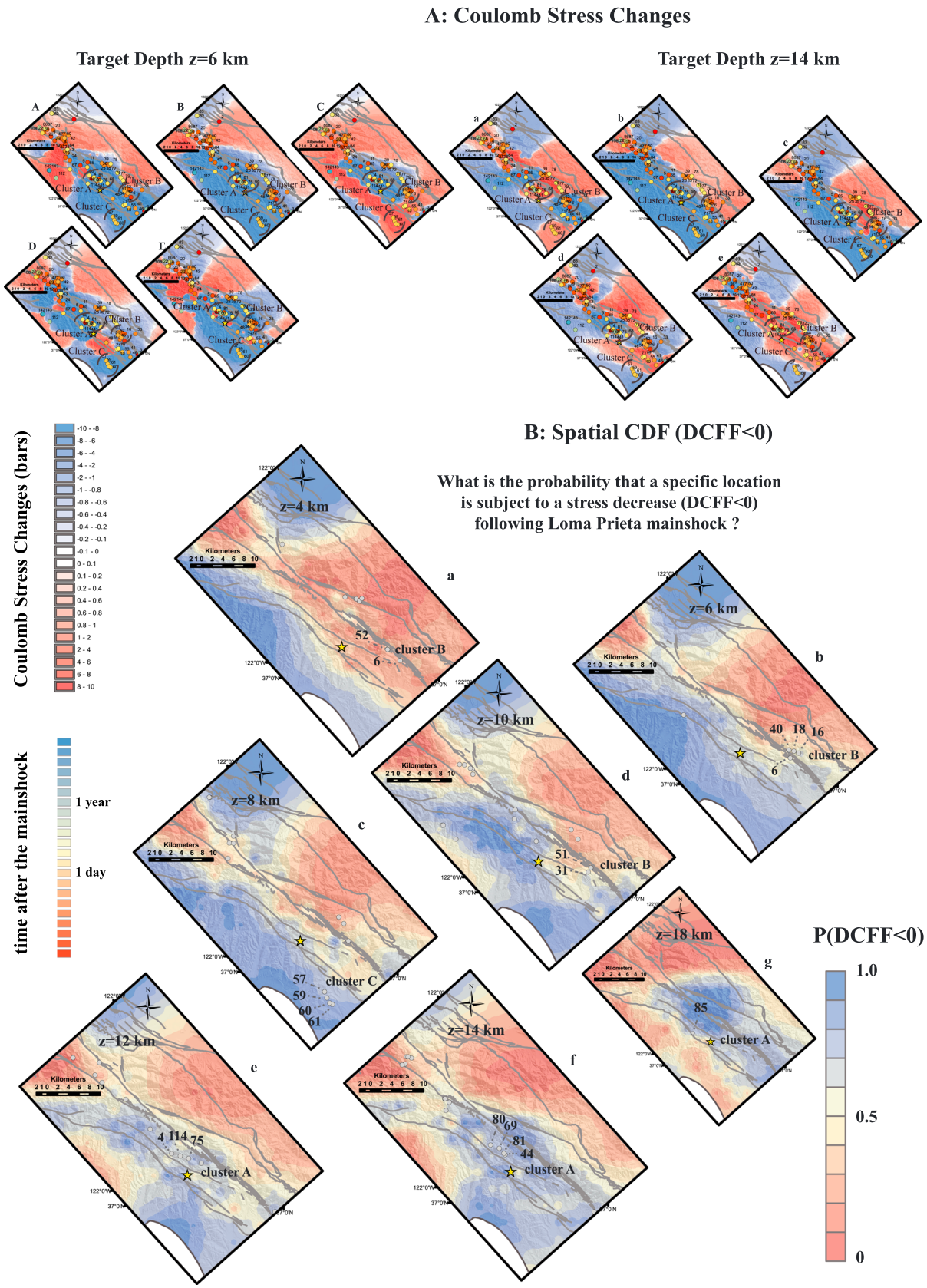

Figure 1

©2014. American Geophysical Union. All Rights Reserved.

shock and that persisted for about 2 years, and (2) the absence of aftershocks on parts of the Loma Prieta rupture plane that slipped during the main shock, as seen in other California main shocks [*Mendoza and Hartzell*, 1988]. We select three aftershock clusters (labeled A, B, and C in Figure 1, panel A) that occurred in calculated stress shadows for studying secondary triggering effects.

In our Coulomb/rate-state (CRS) model framework, the seismicity rate R is a function of a state variable γ that evolves in time under a shear-stressing rate according to the *Dieterich* [1994] equations (see Appendix S1 in the supporting information). We include effects from nine $M \geq 5.0$ Northern California ruptures that occurred between 1980 and 1989 into the state variable (γ_{n-1}) calculation (see Table S1). Aftershock locations are taken from the high precision relocated catalog of *Waldhauser and Schaff* [2008], with uncertainties in the horizontal and vertical direction of approximately 1 km and 2 km, respectively.

The main components of the CRS model implementation are (1) 3-D static stress change calculations with target depth sampled every 0.4 km, (2) rate-state constitutive parameters, stressing rate i, and the term $A\sigma$ (where A is a constant, and σ is a normal stress), and (3) a reference seismicity rate ($M \geq 1.6$) from the period 1974–1980 (Advanced National Seismic Network (ANSS) catalog). We assume uniform reference rates because there is limited information and sparse seismicity in the epicentral area of Loma Prieta main shock before 1980. However, we note that the selection of the background seismicity model is important in physics-based forecasting as in Northern California [*Segou et al.*, 2013] and in other locations [*Hainzl et al.*, 2010]. We calculate the mean Coulomb stress change using all available main shock source models at 3-D points for varying coefficients of friction ($0.2 \leq \mu \leq 0.8$) and the 95% confidence interval. We note that stressing rate $\dot{\tau}$ and the $A\sigma$ term are related through $\dot{\tau} = A\sigma/t_a$ [*Dieterich*, 1994], where t_a is the aftershock duration. In this implementation we choose to fix the stressing rate for the San Andreas Fault Peninsula segment based on *Parsons* [2002] and vary the term $A\sigma$ from 0.2 to 2 bars with a 0.2 bar sampling interval. Although previous studies for California suggest a good fit for $A\sigma = 0.5$ [*Toda et al.*, 2005; *Segou et al.*, 2013], we use 10 different values here to assess sensitivity of this parameter on forecast aftershock rates [e.g., *Hainzl et al.*, 2010].

We use five Loma Prieta source models [*Lisowski et al.*, 1990; *Beroza*, 1991; *Marshall et al.*, 1991; *Steidl et al.*, 1991; *Wald*, 1991] for calculating main shock static stress changes (Figure 1, panel A) because our aftershock clusters lie within ~10 km of the rupture plane, and calculations at these locations might be sensitive to small differences in the source slip distributions [*Simpson and Reasenberg*, 1994; *Steacy et al.*, 2004]. We calculate stress changes on specific planes, based on pre–main shock predominant geology features [*McLaughlin et al.*, 1972; *Clark*, 1981; *Aydin and Page*, 1984; *Segou et al.*, 2013], at varying target depths with spatial resolution in both vertical and horizontal direction 2 km. The predominant geology grid receiver planes are represented by (1) vertical dextral strike slip (strike: N40°W, rake: 180°) for target depths less than 10 km, corresponding to the Santa Cruz Mountains section of the San Andreas Fault, (2) dextral reverse oblique planes (rake 135°) trending N57°W dipping 60°SW that represent the Zayante-Vergeles fault zone, and that mark the merge of the thrust component of the Santa Cruz Mountains section of the San Andreas Fault zone for target depths greater than 10 km. The above interpretation is for the central part of the Loma Prieta rupture, and is based on the Loma Prieta aftershock interpretation of *Dietz and Ellsworth* [1990, 1997]. They find that although there is a diversity of focal mechanisms within the aftershock sequence [see also *Beroza and Zoback*, 1993; *Kilb et al.*, 1997], strike slip faulting dominates the upper 10 km, whereas dextral reverse faulting similar to the main shock mechanism occurs between 10 and 18 km.

Figure 1. Panel (A) Coulomb stress changes following Loma Prieta $M_w = 6.9$ main shock resolved for target depths (A–E) $z = 14$ and (a–e) $z = 6$ km using the source models of (A-a) *Beroza* [1991], (B-b) *Lisowski et al.* [1990], (C-c) *Marshall et al.* [1991], (D-d) *Wald* 1991, and (E-e) *Steidl et al.* [1991] for friction coefficient $\mu = 0.4$. Aftershocks are taken from the relocated catalog of *Waldhauser and Schaff* [2008]; early aftershocks (first day) corresponding to warm colors going to colder ones for longer time intervals (>1 year). The (A–C) aftershock clusters under analysis are identified. Both CRS models are based on a 3-D static stress change calculation sampling target depth interval 2 km taking into consideration varying friction coefficients ($0.2 \leq \mu \leq 0.8$). Panel (B) Map view of the probability that a location is under stress decrease ($P_{DCFF<0}$) following Loma Prieta $M_w = 6.9$ main shock (denoted as *star*) at specific target depths overlaid with the events with $M \geq 3.5$ within each depth range. For calculating this statistical metric we have considered different slip models and varying coefficient of friction ($0.2 \leq \mu \leq 0.8$). We identify the events within each cluster and we present in Table S2 the probability that a specific event location is under stress decrease following the main shock. We observe that the triggering potential of the aftershocks to counteract stress shadow following the main shock; therefore, presenting an improved forecast in CRS-2 implementation, the triggering potential of an earthquake is linked with the severity of the initial stress decrease and from the magnitude of the positive stress changes.

©2014. American Geophysical Union. All Rights Reserved.

We assess parameter sensitivity in Coulomb stress modeling by varying friction coefficients ($0.2 \le \mu \le 0.8$) for each main shock model at each target depth. However, there would be too little time immediately after a main shock to develop complex source models, so a uniform slip model like that of *Lisowski et al.* [1990] (see Figure 1, panel A, b), perhaps with stochastic variations, would be more realistic on operational time scales. For each target depth we map the Spatial Cumulative Density Function (SpatialCDF) that answers the question, *What is the probability that a specific location is subject to a stress decrease* (*DCFF* < 0) *following the Loma Prieta mainshock?* We then focus on the clusters with high probability to be under an initial stress shadow. In Figure 1 (panel A) we present example estimated Coulomb stress changes for target depths $z = 14$ and $z = 6$ km, and for friction coefficient $\mu = 0.4$. In Figure 1 (panel B), we present the SpatialCDF in map view for selected target depths; events within clusters A and C have ~70% and ~80% probability of being under a stress shadow, respectively, whereas for cluster B four out of nine events have probability >50% to be under stress shadow, and they occurred early in the cluster evolution.

We use uniform slip models to calculate secondary stress changes from the smaller magnitude events within our clusters. We estimate slip after *Hanks and Kanamori* [1979] assuming that the moment magnitude equals the local magnitude, the stress drop ($\Delta\sigma$) equals 3 MPa [*Dietz and Ellsworth*, 1997], and a shear modulus of 3×10^{11} dyn/cm^2. Source areas are found with the scaling relation of *Wells and Coppersmith* [1994] for the specific fault rake. We would like to note that stress sources are treated differently from receiver faults in this study. Analytically, both possible focal planes are taken into consideration as possible sources for each event within the CRS-2 model implementation, but we use fixed receiver planes based on our best knowledge of the predominant geology, described in detail at an earlier paragraph of this section, in order to resolve stress changes. We do not expect critical stress perturbations from similar magnitude aftershocks at distances greater than 10 km outside the studied clusters.

In Table S2 we present the seismic parameters and focal mechanisms of the events within each cluster, and in Figure S1 we show cluster cross sections, modified from *Dietz and Ellsworth* [1997], with the available focal mechanisms. Not all focal mechanisms are possible to estimate; in these cases we assign focal mechanisms based on their vicinity with another event within the same cluster.

A cautionary note is in order since there are sources of uncertainty such as the availability of a high-accuracy source model, the focal mechanisms of small magnitude events and short-term incompleteness issues for low magnitude thresholds that although critical to any operational forecast effort, they are not even currently within network capabilities.

Before drawing our final conclusions we test whether it is possible to explain the spatial distribution of aftershock within the stress shadows of the main shock, if we consider afterslip as the driving mechanism. In order to address this matter we estimated the static stress changes from two sources of postseismic deformation cited in relevant literature. According to *Bürgmann et al.* [1997], the main features of postseismic deformation suggest aseismic oblique-reverse on the updip of the Loma Prieta rupture (0–8 km) and thrusting along the Foothills thrust. Especially for the Foothills Thrust, we modeled afterslip between 5 and 7 km depth, where coseismic positive stress changes were estimated [*Parsons et al.*, 1999]. We considered that "reverse slip on the Foothills thrust decays from 45 ± 12 mm/yr immediately after the earthquake to zero by 1992" and that "right-lateral slip on the Loma Prieta rupture surface decays monotonically from 30 ± 10 mm/yr to zero by 1994" [*Segall et al.*, 2000]. We assumed the full-observed postseismic deformation within the first year following the main shock for both cases for modeling afterslip. We find that the event locations in clusters A, B, and C receive stress changes ranging from −0.240 to 0.030, −2.72 to −0.33, −0.0291 to 0.0083 bar and −0.022 to 0.034, −0.0576 to −0.04, −0.0135 to −0.0130 bar from the two aforementioned afterslip sources, respectively. Therefore, we support at this point that the magnitude of the stress changes due to afterslip cannot explain aftershock occurrence inside the stress shadow of the main shock.

3. Results

We present our results in Figure 2 in terms of predicted and observed number of aftershocks with $M \ge 1.6$ between the occurrences of $M \ge 3.5$ sources within each cluster. We compare results derived from the CRS-1 model (stress changes associated with the main rupture only) and the CRS-2 model (updated stress field with stress perturbations imparted by $M \ge 3.5$ aftershocks). Our goal is to evaluate the relative and absolute

©2014. American Geophysical Union. All Rights Reserved.

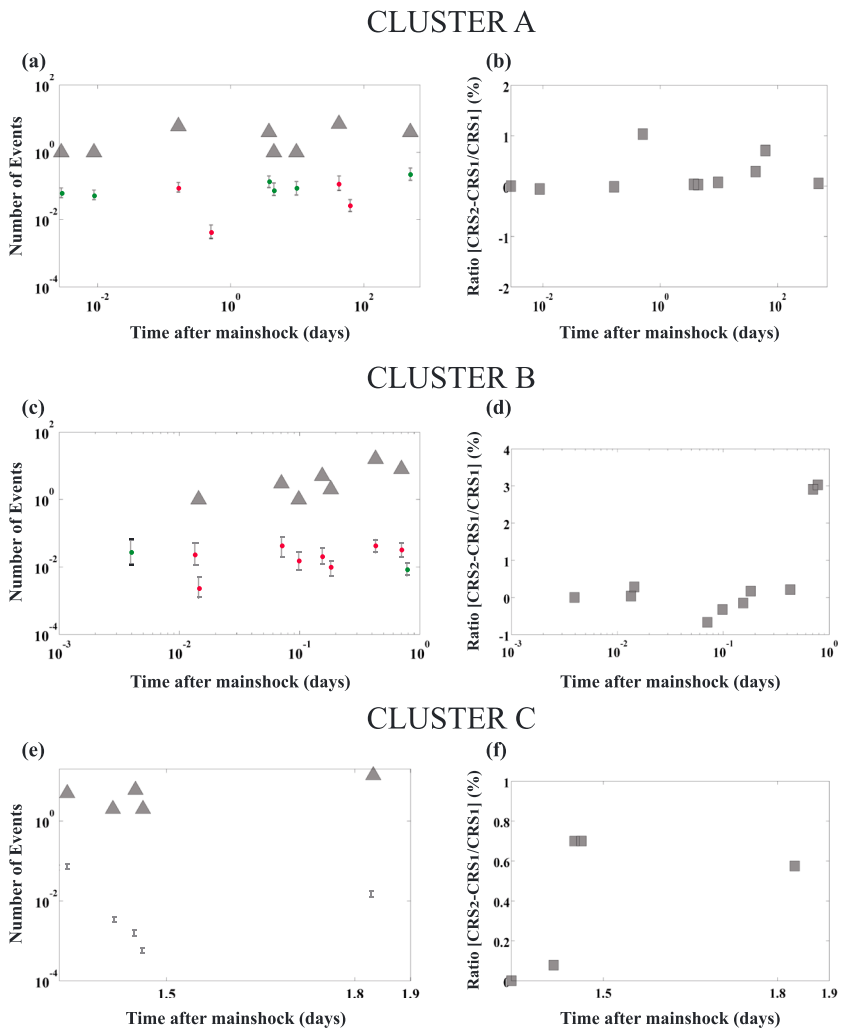

Figure 2. (a, c, e) Observed (triangles) and forecasted number of events with $M \geq 1.6$ plotted between the occurrences of $M \geq 3.5$ sources within each cluster for CRS-1 model (black error bars) that accounts only for the stress changes following $M_w = 6.9$ Loma Prieta (denoted as *star* in Figure 1, panel A) and CRS-2 model (grey error bars), taking into consideration the updated stress field from aftershocks with $M \geq 3.5$. Green and red error bars for clusters A and B correspond to forecasts that pass or not, respectively, the *N* test [*Schorlemmer et al.*, 2007]. We note that all forecasts in cluster C do not pass the *N* test. (b, d, f) Ratio of the difference of number of forecasted events (CRS_2-CRS_1) normalized by the number of events of the CRS-1 model. We observe that CRS-2 model presents little difference, up to 3%, compared with CRS-1 model supporting that the static stress changes from small magnitude events do not play an important role in local stress redistribution. The errors bars represent estimated errors due to the fault constitutive parameters $A\sigma$, which varies between 0.1 and 2 bars in our implementation, fault plane consideration, and varying coefficients of friction ($0.2 \leq \mu \leq 0.8$).

predictive power of physics-based models, focusing on whether the inclusion of stress changes from small magnitude aftershocks represents an improvement.

For cluster A, we consider stress perturbations from nine additional events in the CRS-2 implementation, with an average distance between successive events of 2.16 km. The elapsed time after the Loma Prieta main shock spans from 4 min to 560 days. We find that CRS-1 and CRS-2 forecasts do not significantly differ, and that both models tend to underestimate observed seismicity (Figure 2a). This is partly due to very low reference rates in the epicentral area of Loma Prieta for more than a decade before the main shock [*Dietz and Ellsworth*, 1997; *Harris*, 1989]. The ratio of the difference in forecast events between CRS-1 and CRS-2 models is normalized by the CRS-1 forecast within each cluster (see Figure 2b). This shows that consideration of the secondary stresses leads to only a 1% increase of the number of predicted events.

©2014. American Geophysical Union. All Rights Reserved.

In cluster B, we accounted for stress changes caused by nine events (CRS-2 implementation) that occurred less than 1 day after the main shock and with an average distance between successive events of ~1.2 km. Cluster B lies within ~10 km average distance from the main shock epicenter along strike, and the considered events express slip on mainly right-lateral vertical planes at depths $<$10 km and also oblique-reverse sense of motion at depths $>$10 km. We find that both forecast models, CRS-1 and CRS-2, underestimate the observed number of events, and that both models give similar results (Figure 2c). Consideration of secondary stresses leads to a 3% increase of the number of predicted events, a similar result as was found for cluster A (Figure 2d).

Cluster C includes events that occurred within 2 days after the Loma Prieta main shock, with an average distance between successive events of 0.91 km. This cluster is the most distant from the rupture plane at approximately 12 km. Focal mechanisms suggest a subvertical plane trending N170°E, which is also delineated by the aftershock epicenters. Consideration of secondary stresses again leads to only a 1% increase of the number of predicted events corresponding to the effect of events ID 59 and 60 (Figures 2e–2f).

We assess the consistency of our forecasts in each cluster using the modified *N* test, through the statistical metrics δ_1 and δ_2, (see Appendixes S2-1 and S2-2, respectively) defined in *Zechar et al.* [2010]. During the implementation of this test we have considered the mean forecasted rates of events with $M \geq 1.6$. We find that CRS-1 forecasts are rejected (see "red" error bars in Figure 2) due to underestimation ($\delta_1 \rightarrow 0$) for the all the time intervals of our forecast that Nobs $\neq 0$.

In order to further understand why the CRS-2 model did not sufficiently improve our predictability, we study the time series of cumulative Coulomb stress changes for locations within each cluster where we observe clustered target seismicity that lies in the vicinity of a single event within each cluster. Our aim is to study whether the negative static stress changes following the main shock could be lifted during the cluster evolution from the secondary stress changes. Alternatively stated, we test whether small magnitude events have an important role in the redistribution of stress at a local level. We first focus on two locations within cluster A at the vicinity of events ID 85 and 65. We observe in Figure S2-a_1 that the positive stress changes of events ID 4, 69, 80, 85, and 114 were not sufficient to counter the strong stress shadow (~ $-$35 bars) whereas in Figure S2-a_2 we calculate that secondary static stress changes enhance the initial negative stress change. Similar findings (Figures S2b_{1-2} and S2c) suggest that the small magnitude of secondary stress changes cannot counteract the static stress changes of the main shock, and in some cases aftershocks continue to occur at locations further inhibited. *Woessner et al.* [2011] also concluded that including aftershock stress changes does not improve the predictability of CRS models, even though they incorporated $M \geq 4.5$ events in their analysis. According to *Meier et al.* [2014] recent findings, only one fifth of the 15% of the aftershocks located in the stress shadow of Landers main shock could be explained by static stress triggering, leading the authors to support that "these aftershocks require a different triggering mechanism."

4. Conclusions

Consideration of an updated stress field that uses static stress perturbations of smaller magnitude ($M \geq 3.5$) aftershocks provides negligible improvement (1%–3%) in the predictive power of physics-based forecast models and still cannot explain aftershock clustering within stress-shadowed locations at the near-source region. In the case of the Loma Prieta rupture, where specific aftershock clusters remained active through the entire sequence, we find that secondary static stress changes cannot counteract the initial stress shadow, resulting in continued underestimation of the seismicity rates. This underestimation is further enhanced by the low reference rates observed in the epicentric area of Loma Prieta before 1980. Forecasting aftershock occurrence at near-source areas with negative coseismic stress changes and low reference seismicity rates is clear limitations of stress-based forecasts.

Accounting for secondary triggering effects may become more important with distance away from the rupture plane, since at the near field, positive stress changes from aftershocks cannot counteract the very strong initial stress shadow cast by the main shock. Spatially random aftershock distributions in the near-source region could be revealing dynamic triggering, especially in the stress shadow zone. Judging from their locations along the rupture plane, they may represent low-strength sites close to failure.

©2014. American Geophysical Union. All Rights Reserved.

Optimizing operational physics-based forecast models (CRS) by including perturbations from early aftershocks is similar to including smaller magnitude secondary events in an epidemic-type aftershock sequence (ETAS) model [*Ogata*, 1998]. We should note, however, that the improvements do not share the same spatial component in both cases because ETAS results imply an isotropic rate increase that depends on the distance decay parametrization, whereas CRS modeling reflects the characteristic pattern of stress change increase/decrease lobes. In both cases, the potential spatial extent of the improved forecast is expected to be only a few kilometers, which leads to the conclusion that if we include secondary triggering effects in a given forecast model, then ETAS modeling is more forgiving of location uncertainty because it does not forecast rate decreases. A common requirement for improving both statistical and physics-based forecasters is the need for small magnitude aftershock locations with high accuracy, which are usually underdetected, especially in the near-source region during the first hours after a main shock.

We observe that aftershocks continue to occur in locations where secondary stress changes enhance the initial stress shadow. The above statement in addition with the persistent underprediction by the CRS models, even those that account for secondary triggering effects, points to additional physical processes beyond static stress triggering that cause aftershocks in the near field.

Acknowledgments
The high-precision relocated catalog of Northern California [*Waldhauser and Schaff*, 2008] is available at http://www.ldeo.columbia.edu/~felixw/NCAeqDD/ (last accessed February 2013). The ANSS catalog and USGS Quaternary Fault maps are available at http://earthquake.usgs.gov/monitoring/anss/ and http://earthquake.usgs.gov/hazards/qfaults/ (last accessed February 2013). The authors thank W. Ellsworth and F. Pollitz for their helpful reviews and suggestions.

The Editor thanks Max Werner and an anonymous reviewer for their assistance in evaluating this paper.

References

Aydin, A., and B. M. Page (1984), Diverse Pliocene-Quaternary tectonics in a transform environment, San Francisco Bay region, California, *Geol. Soc. Am. Bull.*, *95*, 1303–1317.

Beroza, G. C. (1991), Near-source modeling of the Loma Prieta earthquake: Evidence for heterogeneous lip and implications or earthquake hazard, *Bull. Seismol. Soc. Am.*, *81*, 1603–1621.

Beroza, G. C., and M. D. Zoback (1993), Mechanism diversity of the Loma Prieta aftershocks and the mechanics of mainshock-aftershock interaction, *Science*, *259*, 210–213.

Bürgmann, R., P. Segall, M. Lisowski, and J. Svarc (1997), Postseismic strain following the 1989 Loma Prieta earthquake from GPS and leveling measurements, *J. Geophys. Res.*, *102*, 4933–4955, doi:10.1029/96JB03171.

Clark, J. C. (1981), *Stratigraphy, Paleontology, and Geology of the Central Santa Cruz Mountains, California Coast Ranges*, 51 pp., *U.S. Geol. Surv. Prof. Pap.*, *1168*, Reston, Va.

Dieterich, J. (1994), A constitutive law for rate of earthquake production and its application to earthquake clustering, *J. Geophys. Res.*, *99*, 2601–2618, doi:10.1029/93JB02581.

Dietz, L. D., and W. L. Ellsworth (1990), The October 17, 1989, Loma Prieta, California, earthquake and its aftershocks: Geometry of the sequence from high-resolution locations, *Geophys. Res. Lett.*, *17*(6811), 1417–1420, doi:10.1029/GL017i009p01417.

Dietz, L. D., and W. L. Ellsworth (1997), Aftershocks of the 1989 Loma Prieta earthquake and their tectonic implications, in *The Loma Prieta, California Earthquake of October 17, 1989—Aftershocks and Post-Seismic Effects*, edited by P. A. Reasenberg, pp. D5–D47, *U.S. Geol. Surv. Prof. Pap.*, 1550-D, Reston, Va.

Felzer, K. R., and E. E. Brodsky (2005), Decay of aftershock density with distance indicates triggering by dynamic stress, *Nature*, *441*, 735–738.

Freed, A. M. (2005), Earthquake triggering by static, dynamic and post-seismic stress transfer, *Annu. Rev. Earth Planet. Sci.*, *33*, 335–67, doi:10.1146/annurev.earth.33.092203.122505.

Hainzl, S., G. Brietzke, and G. Zöller (2010), Quantitative earthquake forecasts resulting from static stress triggering, *J. Geophys. Res.*, *115*, B11311, doi:10.1029/2010JB007473.

Hanks, T., and H. Kanamori (1979), A moment magnitude scale, *J. Geophys. Res.*, *84*(B5), 2348–2350, doi:10.1029/JB084iB05p02348.

Harris, R. (1989), Forecasts of the 1989 Loma Prieta, California, earthquake, *Bull. Seismol. Soc. Am.*, *88*(4), 898–916.

Hill, D. P., and S. G. Prejean (2007), Dynamic triggering, in *Treatise on Geophysics*, vol. 4, Earthquake Seismology, edited by H. Kanamori, pp. 257–291, Elsevier, Amsterdam, doi:10.1016/B978-044452748-6.00070-5.

Lisowski, M., W. H. Prescott, J. C. Savage, and M. J. Johnston (1990), Geodetic estimation of coseismic slip during the 1989 Loma Prieta, California, earthquake, *Geophys. Res. Lett.*, *17*, 1437–1440, doi:10.1029/GL017i009p01437.

Kilb, D., M. Ellis, J. Gomberg, and S. Davis (1997), On the origin of diverse aftershock mechanisms 1989 Loma Prieta earthquake, *Geophys. J. Int.*, *128*, 557–570.

Mallman, E. P., and T. Parsons (2008), A global search for stress shadows, *J. Geophys. Res.*, *113*, B12304, doi:10.1029/2007JB005336.

Marsan, D. (2005), The role of small earthquakes in redistributing crustal elastic stress, *Geophys. J Int.*, *163*, 141–151, doi:10.1111/j.1365-246X.2005.02700.x.

Marshall, A., R. S. Stein, and W. Thatcher (1991), Faulting geometry and slip from co-seismic elevation changes; the 18 October 1989, Loma Prieta, California, *Bull. Seismol. Soc. Am.*, *81*, 1660–16,931.

McLaughlin, R. J., T. R. Simoni, E. D. Osbun, and P. G. Bauer (1972), Preliminary Geologic Map of the Loma Prieta-Mt. Madonna Area, Santa Clara and Santa Cruz Counties, *U.S. Geol. Surv. Open File Rep.*, pp. 72–242, California.

Meier, M.-A., M. J. Werner, J. Woessner, and S. Wiemer (2014), A search for evidence of secondary static stress triggering during the 1992 *Mw*7.3 Landers, California, earthquake sequence, *J. Geophys. Res. Solid Earth*, *119*, 3354–3370, doi:10.1002/2013JB010385.

Mendoza, C., and S. H. Hartzell (1988), Aftershock patterns and main shock faulting, *Bull. Seismol. Soc. Am.*, *78*, 1438–1449.

Ogata, Y. (1998), Space-time point-process models for earthquake occurrences, *Ann. Inst. Stat. Math.*, *50*, 379–402.

Parsons, T., R. S. Stein, R. W. Simpson, and P. A. Reasenberg (1999), Stress sensitivity of fault seismicity: A comparison between limited-offset oblique and major strike-slip faults, *J. Geophys. Res.*, *104*, 20,183–20,202, doi:10.1029/1999JB900056.

Parsons, T. (2002), Post-1906 stress recovery of the San Andreas fault system from 3-D finite element analysis, *J. Geophys. Res.*, *107*(B8, 2162), doi:10.1029/2001JB001051.

Parsons, T., Y. Ogata, J. Zhuang, and E. L. Geist (2012), Evaluation of static stress change forecasting with prospective and blind tests, *Geophys. J. Int.*, *188*, 1425–1440, doi:10.1111/j.1365-246X.2011.05343.x.

©2014. American Geophysical Union. All Rights Reserved.

Richards-Dinger, K., S. Toda, and R. S. Stein (2010), Decay of aftershock density with distance does not indicate triggering by dynamic stress, *Nature*, *467*, 583–586, doi:10.1038/nature09402.

Schorlemmer, D., M. C. Gerstenberger, S. Wiemer, D. D. Jackson, and D. A. Rhoades (2007), Earthquake likelihood model testing, *Seismol. Res. Lett.*, *78*(1), 17–29, doi:10.1785/gssrl.78.1.17.

Segall, P., R. Bürgmann, and M. Matthews (2000), Time-dependent triggered afterslip following the 1989 Loma Prieta earthquake, *J. Geophys. Res.*, *105*(B3), 5615–5634, doi:10.1029/1999JB900352.

Segou, M., T. Parsons, and W. L. Ellsworth (2013), Comparative evaluation of physics-based and statistical forecast models in Northern California, *J. Geophys. Res. Solid Earth*, *118*, 6219–6240, doi:10.1002/2013JB010313.

Simpson, R. W., and P. A. Reasenberg (1994), Earthquake-Induced Static Stress Changes on Central California Faults, *U.S. Geol. Surv. Prof. Pap., 1550-F*, pp. 55–89.

Steacy, S., D. Marsan, S. S. Nalbant, and J. McCloskey (2004), Sensitivity of static stress calculations to the earthquake slip distribution, *J. Geophys. Res.*, *109*, B04303, doi:10.1029/2002JB002365.

Steidl, J. H., R. J. Archuleta, and S. H. Hartzell (1991), Rupture history of the 1989 Loma Prieta California earthquake, *Bull. Seismol. Soc. Am.*, *81*, 1573–1602.

Stein, R. S. (1999), The role of stress transfer in earthquake occurrence, *Nature*, *402*, 605–609.

Toda, S., and R. Stein (2003), Toggling of seismicity by the 1997 Kagoshima earthquake couplet: A demonstration of time dependent stress transfer, *J. Geophys. Res.*, *108*(B12), 2567, doi:10.1029/2003JB002527.

Toda, S., R. S. Stein, K. Richards-Dinger, and S. Bozkurt (2005), Forecasting the evolution of seismicity in southern California: Animations built on earthquake stress transfer, *J. Geophys. Res.*, *110*, B05S16, doi:10.1029/2004JB003415.

Toda, S., R. S. Stein, G. C. Beroza, and D. Marsan (2012), Aftershocks halted by static stress shadows, *Nat. Geosci.*, *5*, 410–413, doi:10.1038/ngeo1465.

Wald, D. J. (1991), Rupture model of the 1989 Loma Prieta earthquake from their inversion of strong-motion and broadband teleseismic records, *Bull. Seismol. Soc. Am.*, *81*, 1540–1572.

Waldhauser, F., and D. P. Schaff (2008), Large-scale relocation of two decades of Northern California seismicity using cross-correlation and double-difference methods, *J. Geophys. Res.*, *113*, B08311, doi:10.1029/2007JB005479.

Wells, D. L., and K. J. Coppersmith (1994), New empirical relationships among magnitude, rupture length, rupture width, rupture area, and surface displacement, *Bull. Seismol. Soc. Am.*, *84*, 974–1002.

Woessner, J., S. Hainzl, W. Marzocchi, M. J. Werner, A. M. Lombardi, F. Catalli, B. Enescu, M. Cocco, M. C. Gerstenberger, and S. Wiemer (2011), A retrospective comparative forecast test on the 1992 Landers sequence, *J. Geophys. Res.*, *116*, B05305, doi:10.1029/2010JB007846.

Zechar, J. D., M. C. Gerstenberger, and D. A. Rhoades (2010), Likelihood-based tests for evaluating space-rate-magnitude earthquake forecasts, *Bull. Seismol. Soc. Am.*, *100*, 1184–1195, doi:10.1785/01200901.

©2014. American Geophysical Union. All Rights Reserved.